

EVIDENCE FOR DOUBLE DIFFRACTION IN pp INTERACTIONS AT 300 GeV/c

A. Firestone, V. Davidson, F. Nagy, C. Peck, and A. Sheng
California Institute of Technology, Pasadena, California 91109

and

F. T. Dao, R. Hanft, J. Lach, E. Malamud, and F. Nezrick
Fermi National Accelerator Laboratory, Batavia, Illinois 60510

and

A. Dzierba
Indiana University, Bloomington, Indiana 47401

and

R. Poster and W. Slater
University of California, Los Angeles, California 90024

December 1974



Evidence for Double Diffraction in pp Interactions at 300 GeV/c.*

by

A. Firestone, V. Davidson, F. Nagy, C. Peck, and A. Sheng

California Institute of Technology, Pasadena, California 91109

F. T. Dao[†], R. Hanft, J. Lach, E. Malamud, and F. Nezrick

Fermi National Accelerator Laboratory, Batavia, Illinois 60510

A. Dzierba

Indiana University, Bloomington, Indiana 47401

R. Poster and W. Slater

UCLA, Los Angeles, California 90024

ABSTRACT

We have observed evidence for the double diffraction process $pp \rightarrow N^*N^*$ at 300 GeV/c. The symbol N^* is here used to refer to the low-mass enhancement which decays into three charged particles (with or without neutrals). The cross section for this reaction is measured to be 0.12 ± 0.05 mb. The cross section for the single beam diffraction reaction, $pp \rightarrow pN^*$, is measured to be 0.82 ± 0.08 mb. These data are in good agreement with the predictions of the factorization hypothesis.

* Work supported by the United States Atomic Energy Commission and the National Science Foundation.

† Present address: Physics Department, Tufts University, Medford, Mass., 02155.

Many of the characteristics of very high energy reactions observed in the CERN-ISR and with the Fermilab 30-inch bubble chamber can be understood in terms of multiperipheral or fragmentation ideas. Certainly a major component of such ideas, especially in reference to diffractive scattering, is the idea of Pomeron exchange. In order to understand the nature of this process, the differential cross section for reactions in which either projectile or target diffracts, e.g. $pp \rightarrow pN^*$, have been studied from threshold up to the highest energies currently available⁽¹⁾. There have thus far been no measurements of the cross sections of the reactions in which both projectile and target diffract in the same event, e.g. $pp \rightarrow N^*N^*$ ⁽²⁾. At low energies it is particularly difficult to isolate a clean sample of such events because the rapidity difference between the target fragmentation region and the beam fragmentation region is small. The current experiment has the advantage that at this very high energy there is a relatively large rapidity gap between the two regions so a clean separation becomes possible. In this work we use the symbol N^* to refer to a low-mass enhancement which decays visibly in the bubble chamber into three charged particles (with or without neutrals).

The data were obtained from 35000 pictures taken with the 30-inch hydrogen bubble chamber exposed to a 300 GeV/c proton beam at the Fermi National Accelerator Laboratory. The results reported on here are based on measurements of 1197 six-prong events, which is about 79% of the total sample in the film. The events have been measured at the Fermilab and details of the scanning, measuring, reconstruction, etc. have been published⁽³⁾.

In this work the measurements of six-prong events are used to isolate a clean sample of double diffraction events. We select those six-prongs with low-mass $p\pi^+\pi^-$ combinations in the target fragmentation region (low momentum in the laboratory frame). These particles are slow in the bubble chamber and

therefore can be measured well. We then calculate the missing mass against this slow system, and select only those events for which this missing or "fast" mass is small as candidates for double diffraction. The observation of six charged particles in the final state thus guarantees that the event is not a single target diffraction event. This method is used because of the unreliability of measurements of fast tracks in very high energy experiments in the bare 30-inch bubble chamber, and the consequent large uncertainties in kinematic fits at these energies. In this way our results are independent of any measurements of the fast system or of any kinematic fits; yet the observed charge and (after the cut is made) low mass of the "fast" system recoiling against the measured "slow" system ensure diffraction of the beam proton.

Figure 1a shows the distribution in $M(p\pi^+\pi^-)$ for all possible $p\pi^+\pi^-$ combinations consistent with ionization. All measured six-prongs were examined on the scan table and the bubble density recorded for all tracks with measured laboratory momenta less than 1.6 GeV/c. Since each positive track is reconstructed as either a proton or a π^+ , there is a theoretical maximum of 24 possible $p\pi^+\pi^-$ combinations per six-prong event, but 76% of these combinations are rejected by ionization inconsistency, observed stopping protons, etc. The distribution in figure 1a is dominated by a large low-mass enhancement centered at about 1.8 GeV. The distribution in figure 1b shows $M(p\pi^+\pi^-)$ with only one $p\pi^+\pi^-$ combination plotted per event. A cut at $M^2(p\pi^+\pi^-) < 40 \text{ GeV}^2$ has been imposed⁽⁴⁾, and for those events with more than one combination satisfying this cut, that $p\pi^+\pi^-$ combination with the lowest $|t|$ from target to $p\pi^+\pi^-$ system is chosen. Just as for figure 1a, the distribution in figure 1b is dominated by a low-mass enhancement centered at about 1.8 GeV.

Figure 1c shows the distribution in the square of the missing mass recoiling against this $p\pi^+\pi^-$ system whose invariant mass distribution was shown in figure 1b. A clear low-mass signal above the dashed background curve can be seen in the region less than 40 GeV^2 . There are 17 events with negative missing mass squared,

i.e. missing momentum greater in magnitude than missing energy. These 17 events were judged to have wrong mass interpretations chosen and were rejected. Figure 2 is a plot of the laboratory longitudinal rapidity of the "fast" or missing system versus the mass of this "fast" system for all events shown in figure 1b. The low-mass high-rapidity enhancement in the "fast" system can be seen at the top of the distribution. We point out that the striking correlation between rapidity and the square of the missing mass is due to the restricted range of transverse momenta.

To isolate the double diffraction signal we now impose the cut that the square of the missing or "fast" mass be less than 40 GeV^2 , and in addition remove the five events shown in figure 2 with missing mass squared less than 40 GeV^2 but with "fast" rapidity less than 3. These five events are those for which the selected "slow" $p\pi^+\pi^-$ combination is in the beam rather than the target fragmentation region, and are therefore unreliable. There remains a sample of 118 events which includes the double diffraction signal plus background. Figure 3a shows the distribution in the laboratory longitudinal rapidity for the 118 selected events. For each event two points are plotted: the rapidity of the selected "slow" $p\pi^+\pi^-$ system and the rapidity of the "fast" system recoiling against it. Every event contributes one count to each of the two enhancements. There is a clean separation on the average of four units in rapidity between the two enhancements.

We have studied the decay characteristics of the slow $p\pi^+\pi^-$ system for the double diffraction sample, and find that the $p\pi^+$ and $p\pi^-$ mass distributions (not shown) are dominated by low-mass enhancements in agreement with low energy results and with the $p\pi^+\pi^-$ system studied in four-prong events at $200 \text{ GeV}/c$ ⁽⁵⁾. The $\pi^+\pi^-$ mass distribution (not shown) is heavily peaked at the low-mass end of the spectrum with most of the events falling below the ρ . There is no evidence for strong production of either $\rho(765)$ or $f(1260)$, in good agreement with results

at 200 and 24 GeV/c^(5,6). The t -dependence of the data, where t is the square of the four-momentum transfer from target to slow $p\pi^+\pi^-$ system, is exponential and shows a slope of 7.4 ± 1.2 (GeV/c)⁻².

In order to estimate the cross section for double diffraction, several corrections are necessary. The first of these is represented by the dashed curve shown in figure 1c. This curve represents our estimate of the background under the signal in the distribution of the square of the missing mass against the slow system. Its shape has been determined from the data by selecting all non-diffractive three-particle systems with the "wrong" charge (i.e. +++ or +--) in the 6-prong and 8-prong events, requiring this charged system to be low-mass ($M^2 < 40$ GeV²), and then calculating the square of the missing mass against this wrong-charge non-diffractive system. This shape is then normalized to the observed number of events in the region $40 < M^2 < 80$ GeV². There is a signal of 56 ± 16 events above the background where the quoted error also includes the uncertainty in the background. A similar background subtraction must be performed in the target fragmentation region, leaving a signal of 27 ± 7 events. On the basis of the work reported in reference 3, these 27 events correspond to a cross section of 0.14 ± 0.04 mb. This cross section represents the process in which the target diffracts into a $p\pi^+\pi^-$ system with invariant mass squared less than 40 GeV², and the beam forms a low-mass system (M^2 also less than 40 GeV²), which contains three charged particles (2 positive and 1 negative), and may also include neutrals. This low-mass system formed in the beam fragmentation region contains $p\pi^+\pi^-$, but also includes other states, e.g. $p\pi^+\pi^-\pi^0$, $\pi^+\pi^+\pi^-n$, etc. A partial separation of these states (with large uncertainties) may be obtained thru the use of kinematic fit data. This has been done in two experiments at 200 GeV/c. In a comparison of the inclusive reaction $pp \rightarrow pX$ in the four-prong events with

the four-constraint exclusive reaction $pp \rightarrow pp\pi^+\pi^-$, Whitmore⁽⁷⁾ concludes that only about 35% of the low-mass peak in the inclusive distribution of missing mass against the slow proton is due to the four-constraint reaction, i.e. to the final state $p\pi^+\pi^-$. Similarly, Winkelmann, et al.⁽⁸⁾, in a 200 GeV/c π^-p experiment concluded that the cross section for proton dissociation into $p\pi^+\pi^-$ was only 180 $\mu\text{b.}$ out of a total of 790 $\mu\text{b.}$ for proton dissociation into three charged particles (with or without neutrals) for a ratio of 23%. Both results have large errors, due in part to the uncertainties in kinematic fits at Fermilab energies.

In the current work we do not rely on this separation by kinematic fits, but use the cross sections for which the symbol N^* refers to all decays into three charged particles (with or without neutrals). Therefore our measured cross section requires no correction for the beam vertex, but it excludes the cross sections for $p \rightarrow p\pi^+\pi^- + \text{neutrals}$ and $p \rightarrow \pi^+\pi^+\pi^- + \text{neutrals}$ at the target vertex, and it also includes contamination from events in which the true target fragmentation mass squared (including neutrals) is greater than 40 GeV^2 , but the charged-mass-squared at this vertex is less than 40 GeV^2 . These two effects cancel to some extent.

In order to determine the missed portion of the cross section for $p \rightarrow \pi^+\pi^+\pi^- + \text{neutrals}$ at the target vertex, we perform a calculation in which neutrons with the same transverse momentum and longitudinal rapidity distributions as observed protons are generated, added to the observed events with low-mass $\pi^+\pi^+\pi^-$ systems, and these "expanded" events are processed the same as real events but with the neutron included in the "slow" system. The loss of double diffraction events with $p \rightarrow \pi^+\pi^+\pi^- + \text{neutrals}$ in the target fragmentation region is 8% of the observed signal. The contamination from events, whose true target fragmentation mass squared (including neutrals) is greater

than 40 GeV^2 , we estimate thru a Monte Carlo calculation in which we assume that π^0 's are distributed in longitudinal rapidity and transverse momentum the same as charged pions, and that the average number of π^0 's per six-prong event is 3.8 ± 0.4 , as determined from a study of γ conversions in the bubble chamber⁽⁹⁾. The same Monte Carlo calculation simultaneously gives the correction for improperly excluded events with π^0 's in the target fragmentation region, i.e. for $p \rightarrow p\pi^+\pi^- + \text{neutrals}$. This calculation shows that 19% of the observed signal is in fact contamination. Thus the cross section for the double diffraction reaction $pp \rightarrow N^*N^*$, where each N^* decays into three charged particles (with or without neutrals) is $0.12 \pm 0.05 \text{ mb}$. The quoted error includes our estimate of the uncertainties introduced by the background subtraction and also the uncertainties introduced by the corrections for neutrals.

In order to compare our result with the predictions of the factorization hypothesis, it is necessary to obtain an estimate of the cross section for single diffraction at $300 \text{ GeV}/c$. This is best done thru a study of the missing mass against a slow identified proton in the four-prong events. Figure 3b shows the distribution in the square of the missing mass against the proton for a sample of 1168 measured four-prongs in this experiment. A cut has been made that the measured proton momentum be less than $1.6 \text{ GeV}/c$. All four-prong events have been looked at on the scan table and the bubble density of all tracks with less than 1.6 GeV measured laboratory momentum has been recorded. In this region identification of the proton by ionization is quite reliable. A clear low-mass signal can be seen in the region less than 40 GeV^2 . In addition there are 48 events with missing mass squared less than -40 GeV^2 . These 48 events were judged to be events in which the "slow proton" has been incorrectly identified, and are rejected⁽¹⁰⁾. The remaining 259 events in the region below 40 GeV^2 include the signal for single diffraction of the beam proton into

three charged particles (with or without neutrals) plus background, and is exactly analogous to the beam diffraction signal in the six-prong case shown in figure 1c. In this case the dashed curve represents an estimate of the background, whose shape is determined from the distribution in the square of the missing mass against a negatively charged track of momentum less than 1.6 GeV in the four-prong events. This shape is then normalized to the observed data in the region from 40 GeV^2 to 80 GeV^2 . There is a signal of 189 events above the background. On the basis of the work reported in reference 3, these 189 events correspond to a cross section of $0.82 \pm 0.08 \text{ mb}$. This should be compared to the value of $0.79 \pm 0.14 \text{ mb}$. for this process found by Winkelmann, et al. ⁽⁷⁾ in π^-p interactions at 200 GeV/c. The t -dependence of the enhancement region, where t is the square of the momentum transfer from target proton to recoil proton shows a slope of $10.4 \pm 0.8 (\text{GeV}/c)^{-2}$. The correction for beam diffraction where the recoil proton has a momentum greater than 1.6 GeV/c is negligible.

The prediction of the factorization hypothesis is that

$$\sigma_{\text{DD}}(\text{predict}) = \frac{(\sigma_{\text{SD}})^2}{\sigma_{\text{EL}}}$$

where σ_{SD} is the single vertex diffraction process measured in the four-prongs (beam diffraction), and σ_{EL} is the pp elastic scattering cross section at 300 GeV/c, which has been measured to be $7.89 \pm 0.53 \text{ mb}$. ⁽³⁾. Thus $\sigma_{\text{DD}}(\text{predict}) = 0.09 \pm 0.02 \text{ mb}$., which is in reasonable agreement with our measured value of $0.12 \pm 0.05 \text{ mb}$.

We thank the staffs of the accelerator, Neutrino Lab., 30-inch Bubble Chamber, and Film Analysis Facility at the Fermi National Accelerator Laboratory for their help with the experiment. We also thank Tom Clark for his excellent work on the ionization.

Footnotes and References

- (1) See, for example, G. A. Smith et al., Physics Rev. 123, 2160 (1961); G. Alexander et al., Phys. Rev. 154, 1284 (1967); S. P. Almeida et al., Phys. Rev. 174, 1638 (1968); Z. Ming Ma et al., Phys. Rev. Letters 23, 342 (1969); R. A. Jespersen et al., Phys. Rev. Letters 21, 1368 (1968); and J. Whitmore, Diffraction Dissociation in pp Interactions at NAL, Particles and Fields - 1973, AIP Conference Proceedings No. 14, AIP New York (p. 371) 1973, and references contained therein.
- (2) A paper by L. Baksay et al., (Measurements of $pp \rightarrow (p\pi^+\pi^-) + X$ at the CERN ISR: Scaling Tests and Evidence for Double Excitation) was presented to the XVII International Conference on High Energy Physics, London, July, 1974, which reported a signal for double excitation, but no cross sections were reported in that work.
- (3) A. Firestone et al., Phys. Rev. D10, (1974).
- (4) The choice of 40 GeV^2 as a cut is dictated by the resolution in the missing mass against the slow system, which is about 1.5 GeV. The expected symmetry of the pp system is demonstrated by the fact that an ideogram of $M^2(p\pi^+\pi^-)$, with the error on the missing mass, plus background, is an excellent fit to the data shown in figure 1c.
- (5) M. Derrick et al., Phys. Rev. Letters 32, 80 (1974).
- (6) M. Idshok et al., Nucl. Phys. B53, 282 (1973).
- (7) J. Whitmore, see reference 1.
- (8) F. C. Winkelmann et al., Diffraction Dissociation in 205 GeV/c π^-p Interactions, Particles and Fields - 1973, AIP Conference Proceedings No. 14, AIP New York (p. 359) 1973.
- (9) A. Sheng et al., pp Interactions at 300 GeV/s: γ and Strange Particle Production, submitted to Phys. Rev. 1974.
- (10) These events with negative missing mass squared generally involve highly dipped slow pions which cannot be reliably separated from slow protons by ionization information.

Figure Captions

- Figure 1: (a) Distribution in $M(p\pi^+\pi^-)$ for all combinations in the six-prongs consistent with ionization.
- (b) Distribution in $M(p\pi^+\pi^-)$, one combination per event with $M^2(p\pi^+\pi^-) < 40 \text{ GeV}^2$, and the combination with lowest $|t|$ chosen.
- (c) Distribution in the square of the missing mass against the selected $p\pi^+\pi^-$ system, whose mass distribution is shown in figure 1b.

Figure 2: Plot of the laboratory longitudinal rapidity versus the square of the mass of the missing or "fast" system recoiling against the selected $p\pi^+\pi^-$ system, for all events with $M^2(p\pi^+\pi^-) < 40 \text{ GeV}^2$ as shown in figure 1b.

- Figure 3: (a) Distribution in the laboratory longitudinal rapidity of both the selected $p\pi^+\pi^-$ system and the missing or "fast" system for those events with both $M^2(p\pi^+\pi^-)$ and missing mass squared $< 40 \text{ GeV}^2$. Each event has two points plotted, one each in the beam and target fragmentation regions.
- (b) Distribution in the square of the missing mass against a slow identified proton with momentum less than $1.6 \text{ GeV}/c$ for the four-prong events.

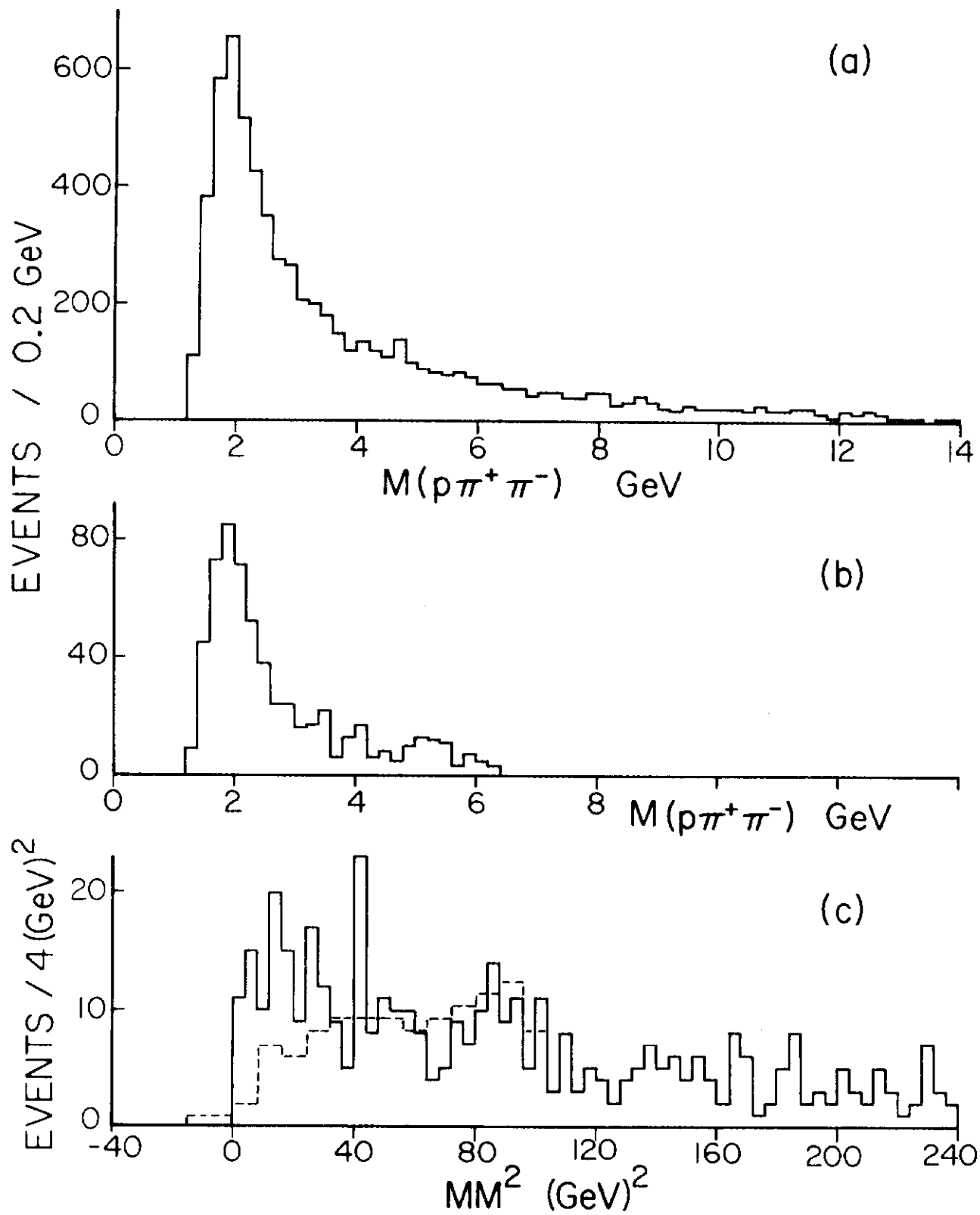


Figure 1

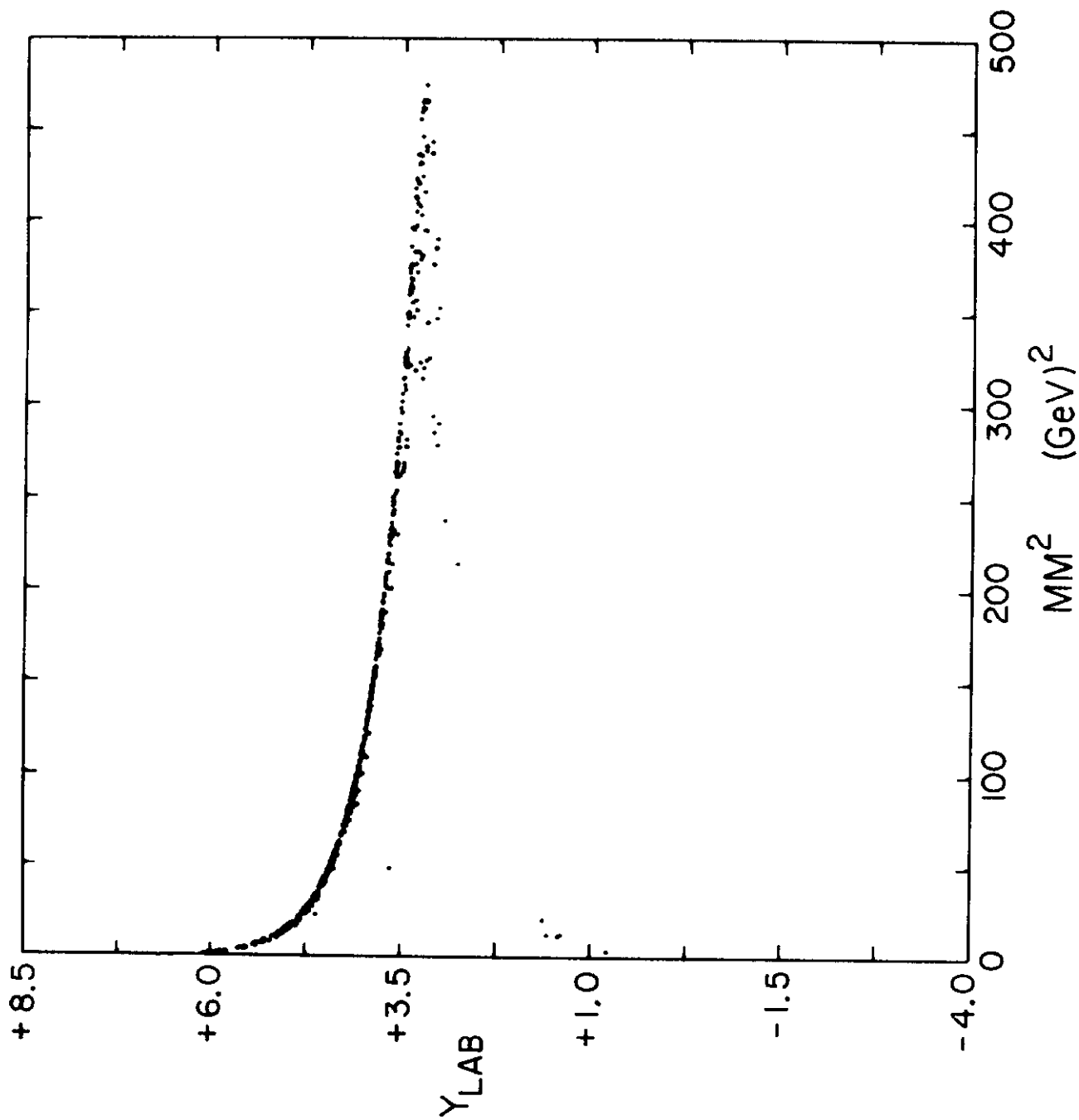


Figure 2

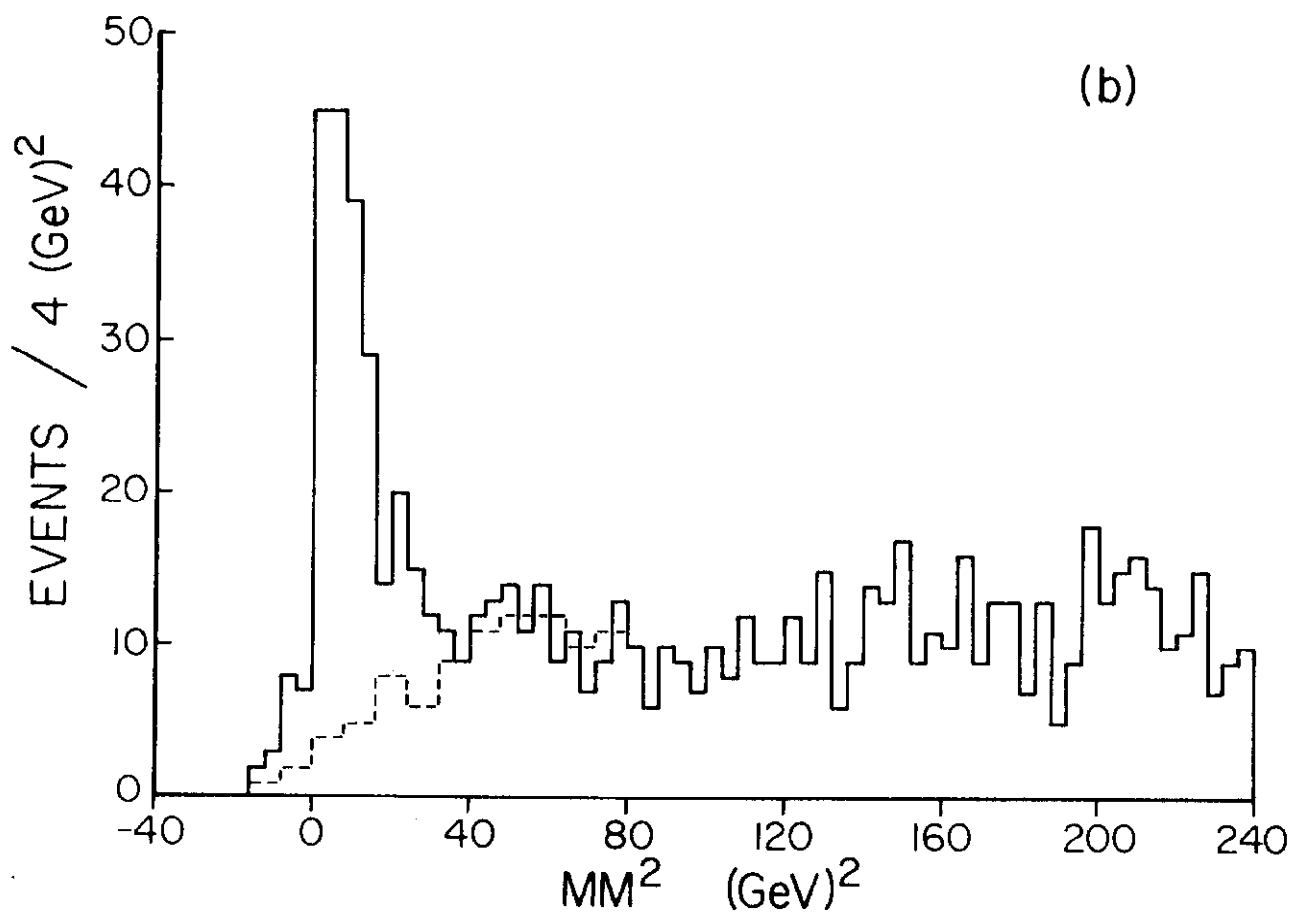
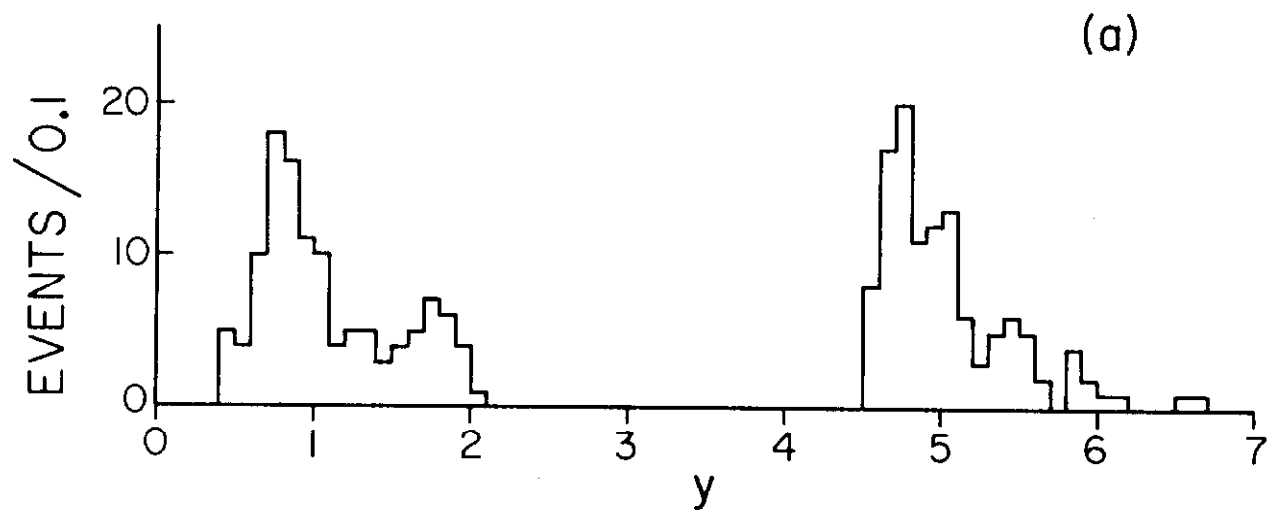


Figure 3